Arboriculture & Urban Forestry 2020. 46(5):321–332

Strain Patterns Across the Root-Stem Transition Zone in Urban Trees

By Kenneth E. Beezley, Gregory A. Dahle, Jason Miesbauer, and David DeVallance

Abstract. Trees are subjected to mechanical loading during their life span or face premature mortality. The strain resulting from loads intercepted by the canopy and transferred throughout the tree is of significant importance, not only for the survival of the tree, but for the safety and well-being of the human population found in close proximity. To test the function of tree orientation to an applied load, static load tests were conducted on 15 mature pin oak trees (*Quercus palustris* Muenchh.). We applied the static load tests to tilt the trees 0.1° from natural position. We used a digital image correlation system to map strain in the leeward, windward, and tangential roots in the root-stem transition zone. Results indicate that mean maximum strain magnitudes are similar in the leeward and windward orientations and lower on the tangential orientation. The leeward orientation experienced compressive strain, the windward orientation experienced tensile strain, and the tangential orientation had both tensile and compressive strain. This information provides the arboricultural and plant science sectors with a better understanding of how loading force moves through trees and will further enhance tree risk assessment and root zone management protocols.

Keywords. Bending Moment; Digital Image Correlation; Static Load Test; Strain; Tree Stability.

INTRODUCTION

Trees have the ability to manage strain (ε) induced from an array of naturally occurring environmental and man-made stresses placed upon both aboveground parts (leaves, branches, woody tissue) and below ground in the structural root support system. Neild and Wood (1999) describe the two main principles of plant growth as the economy of nutrients for light competition and the reaction of the plant to loading stress by the forming of reactive tissue material in areas where strain is greatest. The response of trees to external loading events, of which wind is the single most abiotic destructive mechanism (Niklas 1992; James et al. 2006), is important to understanding tree stability, especially during formal tree risk assessments. Trees are prone to failure as a result of elevated and sustaining winds (James et al. 2014) as well as short, sporadic wind gusts (Coder 2008). In many cases, however, these failures may not be instantaneous (Hale et al. 2010). Research has shown that trees manage stress and the resulting ε across various parts of their architecture through mass damping (James 2003; Moore 2014), shedding of woody parts (James et al. 2006), bending of stems and branches (Brudi and van Wassenaer 2002; Dahle and Grabosky 2010), stem deflection and tilt (Neild and Wood 1999; James et al. 2013a), root-plate tilt (Jonsson et al. 2006; James et al. 2013b), root anchorage (Dupuy et al. 2005), soil-root interactions (Genet et al. 2005), and adaptive growth (Niklas 1992; James 2003). However, there is limited knowledge of how loading force, stress, and resulting ε is transferred from the main stem into the root zone (Beezley et al. 2020).

With the recent increase of catastrophic weather (wind or ice) events in the USA, Europe, and Australia (Moore and Maguire 2004; Yang et al. 2014), liability concerns arising from the retention and preservation of large amenity trees is of increasing concern. As more managed trees are found in populated areas, arborists and urban foresters are faced with the task of determining whether a tree should be removed to limit the risks associated with failure (Dahle et al. 2014). Predisposing factors can increase the likelihood of tree failure during wind events even under

Figure 1. Elevated radial growth and increased diameter at the base of an elm tree.

mild wind and weather conditions (Dahle and Grabosky 2009; Kane 2014; Smiley et al. 2014; Dahle et al. 2017). Some of the predisposing factors include: prior root damage from wind (James et al. 2013b); unstable soil conditions and compromised soil properties (Gibbs and Greig 1990; Genet et al. 2005); and intrusion of the root zone resulting from construction (Moore 2014; Smiley et al. 2014). There is a lack of empirical data (Kane and Clouston 2008; Dahle et al. 2014) on tree stability, therefore limiting tree risk assessors' ability to make informed judgments on the stability of amenity trees.

Root wood develops from a different tissue than stem wood (Esau 1977; Kozlowski and Pallardy 1997). The root-stem transition zone (RSTZ) is the area where root tissue joins stem tissue and is associated with an area of elevated radial growth (Figure 1). Limited literature is available that discusses the RSTZ. This region could be considered somewhat analogous to the branch collar, which is comprised of both branch and stem wood. Yet the branch collar is comprised of the same tissue type. Fayle (1983) defines a stem-root junction as the area at the intersection of the main stem plate and structural roots, near the soil line, where a hinge point can be found after uprooting. After tissue convergence from root to stem, the base of trees experience increased radial growth (James 2003) from canopy stress compared to the bole (main stem), as seen by an apparent swelling effect (Figure 1). This swelling phenomenon is thought to be the result of increased torsional strain at the base of the tree (James 2003). The zone of rapid taper (ZRT) refers specifically to the region within the roots where the stem diverges into large structural roots and rapidly tapers into smaller diameter roots (Lyford and Wilson 1964). Typically, the ZRT is found within 2 m horizontally at the base of the tree. For this study, the term root-stem transition zone was applied to the area which includes the base of the stem, the stem-root-collar, and the zone of rapid taper (Figure 2).

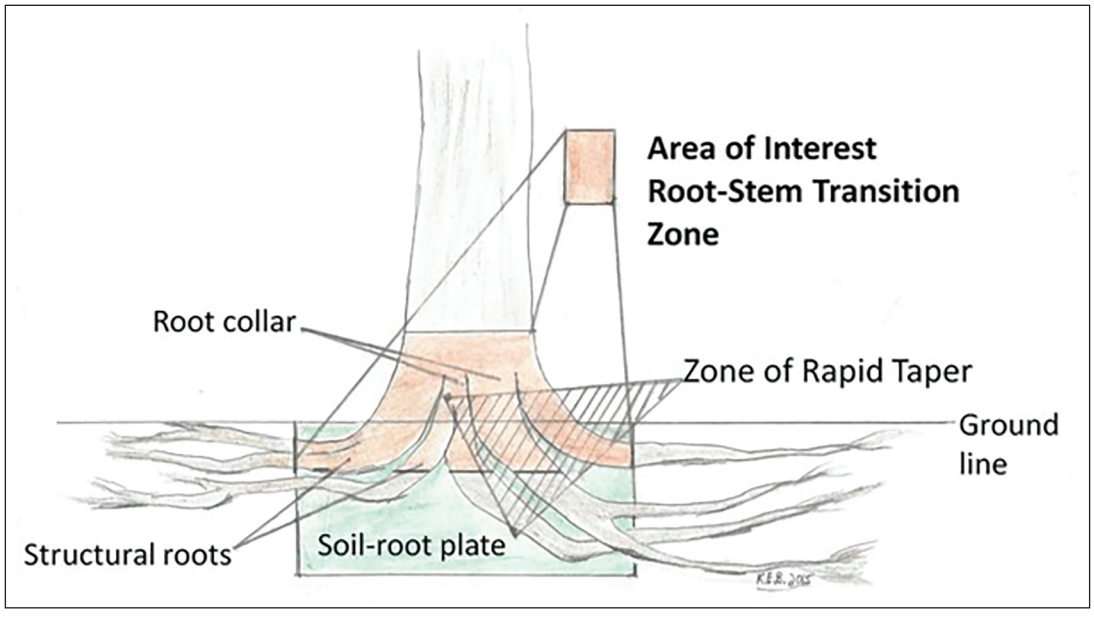

Figure 2. The root-stem transition zone (RSTZ).

Mechanical Loading and Strain

Forces (static or dynamic) are intercepted in the crown, transferred along the stem, and create a turning moment at the stem base that is resisted by wood in the RSTZ (James et al. 2013a, 2013b). Neild and Wood (1999) report that as a tree bends, roots flex because the attachment to the ground is rigid. However, there is currently no supporting evidence into the amount or direction of strain across the RSTZ.

Stress (force per unit area) and strain (deformation) are induced by loading a material or structure. If the loading and resulting strain is below the elastic yield point, the material will return to the original shape when the load is removed (Niklas 2002). As load increases and deformation exceeds the material's elastic yield point, plastic deformation occurs, and the material will not return to its original dimensions (Burgert 2006).

Static pull tests have been implemented on open-grown urban trees to measure the amount of force required to pull trees to failure (Peltola 2006; James et al. 2013a; Smiley et al. 2014), test the effects of root loss on short-term tree stability (Smiley et al. 2014), and to estimate overall tree stability during tree risk assessments (Brudi and van Wassenaer 2002; James et al. 2013a; Sebera et al. 2014). The static pull test approach was first described by Coutts (1983) in forestry research, where a steadily increasing force is applied on selected trees until a target displacement or load is reached or failure occurs. Although static load trials do not fully consider all the dynamic parameters of wind loading (Moore and Maguire 2004; Peltola 2006; Kane and Clouston 2008), including torsion (Dahle and Grabosky 2012; Moore 2014), these tests are suitable to develop baseline information on how loading can move in trees (Dahle 2017).

Various tools used to measure strain in living trees include strain gauges, transducers, and elastometers (James et al. 2018). Recently, researchers have utilized digital image correlation (DIC) techniques to nondestructively test two- and three-dimensional surface deformation (Sebera et al. 2014, 2016; Dahle 2017). DIC has an advantage of mapping strain within the field of view on the object's surface rather than the specific predetermined site where a strain gauge or elastometer is affixed. Additionally, DIC can provide three-dimensional direction vectors. DIC maps deformation and movement by tracking the three-dimensional distance between dots or speckling painted directly on the object's surface. Sebera et al. (2014, 2016) reported that DIC and elastometers provided the same values at lower loading levels when applied directly on the xylem after the phloem was removed. Dahle (2017) has found the application of DIC strain mapping can be successfully used to nondestructively observe strain patterns in trees by using strain on the bark (outer phloem) as a surrogate for strain in the xylem. Incorporating DIC with static load tests will allow researchers to better understand how loads move through trees and thus provide insight into tree stability.

The primary aim of this research was to determine if ε could be measured in the RSTZ to evaluate how mechanical loads are transferred from the stem into the root system. Secondarily, we aimed to determine the type of strain (compression vs. tension) that is induced in the RSTZ and if the magnitude of strain differs by the direction of root growth in relationship to the direction of loading. This research will also provide additional knowledge to arborists and urban forest managers on this important region of a tree in terms of overall stability.

MATERIALS AND METHODS

Fifteen mature pin oak (*Quercus palustris* Muenchh.) trees located on the Evansdale Campus of West Virginia University Morgantown, WV, USA, were subjected to static loading tests between 28 May 2015 and 24 June 2015. The trees were in a flat lawn setting in close proximity to other pin oak trees, sidewalks, or a parking lot (Figure 3). The pin oak tree population

Figure 3. Sample pin oak trees.

ranged in age from approximately 35 to 45 years. The root-stem transition zone was visible prior to the initiation of the study.

To evaluate how force moves into the root system in relation to the direction of loading, 3 roots per test tree were examined. The root orientations were labeled as follows: leeward roots in the direction of the pulling force; windward roots in the opposite direction of the pulling force; and the tangential roots located perpendicular to the direction of the pulling force. Tangential roots could be found on either side of the pulling direction, as depicted by root morphology or physical limitation.

An Air Knife (Allison Park, PA, USA) was used to excavate the root zone adjacent to the base of each tree. First order roots were exposed for 1 m distally from the base of each tree trunk to a depth of approximately 15 cm below grade. Soil excavation was required to expose the root tissue surface for applying the paint for DIC measurements. Fine woody roots were removed with small hand pruners to provide a direct line of sight to the exposed structural roots.

DIC imagery requires a moderately even surface, as thick ridges or deep furrows create a shadowing effect and obstruct the view from one or both cameras. Some of the larger roots had deeply furrowed areas on the RSTZ, and the thick bark ridges (primary phloem) were reduced by means of a draw knife. Care was taken to avoid damaging the secondary phloem. After initial surface preparation, a white background was applied using a flat, nonglossy paint, followed by a stochastic black speckling pattern. After the paint was allowed to dry, reference marks were placed with a permanent marker at 2.5-cm increments along the main axis of the root, starting near the top edge of the painted RSTZ and continuing distally along the main root (Figure 4).

As the roots were not perfectly in line with or perpendicular to the direction of pull, root divergence was a measurement (in degrees) of how a root aligned with the pulling direction. Specifically, root divergence was calculated as the number of degrees (using a compass) that the general direction of root growth differed from the line of pulling (leeward and windward). In the case of tangential roots, root divergence was calculated as the number of degrees from 90° perpendicular to the direction of pull. Soil moisture was measured at three locations, one each on both sides of the given root and one on the distal end.

Figure 4. RSTZ and root prepared for sampling with painted surface and 2.5-cm reference lines on root.

Readings were taken during the same day of sampling for each tree using a Campbell Scientific HydroSense soil moisture probe (Campbell Scientific, Logan, UT, USA) and then averaged.

The static pull line was secured in the tree using a webbed sling that was placed below any codominant branching or lateral limbs that would affect the pulling process (Beezley et al. 2016). A 44-kN capacity load cell (Interface, Scottsdale, AZ, USA) recorded the applied load. The height of the pulling line attachment and the stem diameter at the point of attachment were measured and recorded. A 44-kN capacity electric winch (Warn Industries, Inc., Clackamas, Oregon, USA) was attached to the base of the anchor tree using a webbed sling.

The tilt of the tree stem was measured using a 22.9-cm-long digital level (Husky, Atlanta, GA, USA) that was mounted on 2 aluminum nails. The center of the level was 42.5 cm above the ground, 180° opposite of the pulling direction. A digital video recorder was positioned to record the measurement of the digital level and to capture audio during each pulling trial for use in post processing. The trees were pulled to a stem deflection to 0.1° from natural lean. Figure 5 displays the static loading setup used for this research. Bending moment was calculated as $M_{Bend} = [\text{Cos}\ \theta \times F] \times \text{Height}_A$, where θ is the rope angle, F is the applied

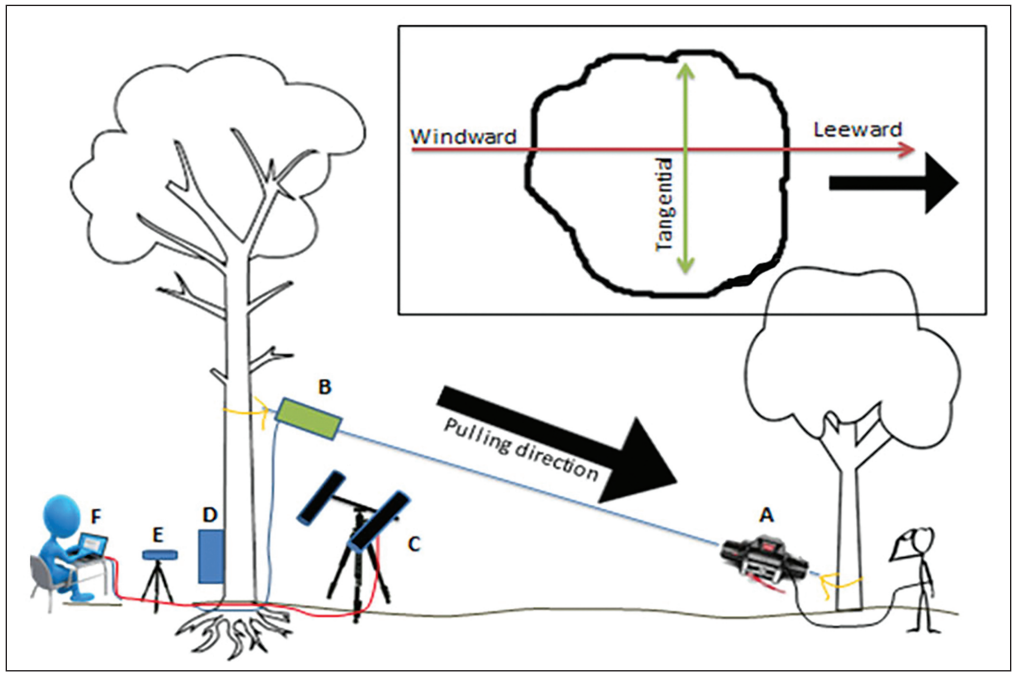

Figure 5. Diagram of static pull test applied to induce a 0.1° inclination for strain measurement across the RSTZ. Winch (A), load cell (B), DIC camera system (C), digital level (D), video recorder (E), and DIC data acquisition station (F).

force (N), and $Height_A$ is the attachment height of the rope above ground level. Each pull was divided into 5 time intervals: one second after start, first quarter, pull midpoint, third quarter, and end (0.1°). M_{Bend} was calculated at each of these 5 intervals.

Initial setup and calibration of the ARAMIS DIC camera system was carried out using a working distance (d) of 180 cm and distance of 60 cm between the two cameras. The DIC system was calibrated prior to initial trials to a calibration deviation of 0.3 and recalibrated as needed. Data was recorded at 2 frames per second. Images were acquired at 2448 × 2050 pixels with a resolution of 72 pixels per inch. The facet size was 20 × 20 pixels with a step size of 15. Linear strain was computed with a 7 × 7 field with a validity quote of 55.5%. The intersection deviation was maintained below 0.03, which provided an accuracy of 0.03 ± 0.003%.

Active Pulling Process

The winch line was retracted until the digital level reached 0.1° inclination. A total of 6 pulls were conducted per tree. Two pulls per root type (windward, leeward, and tangential) were performed, and on each pull the DIC camera was oriented either at the top face (parallel to soil horizon) or side face (perpendicular to soil horizon) of the specific roots.

Digital Image Correlation Processing

As each root was slightly different, the reference tick marks (3 cm apart along the RSTZ) were used to establish a reference point so a comparison between roots could be made. The strain map of the root (Figure 6A) was rotated 90° about the vertical (Figure 6B and 6C), and two straight edges were drawn along the top edge of the structural root and main stem (Figure 6C). The intersection of lines was designated as the zero reflection point. Tick marks moving up the stem from point 0 toward the crown were designated with positive values, while the marks moving toward the root tip were designated with negative values (Figure 6D).

Strain (major/tension, minor/compression) was measured on each reference mark and exported as a text file for analysis. Maximum strain was analyzed from each sampled location on the RSTZ by means of selecting the absolute value of strain (major or minor) at each location. For example, at a given location on the RSTZ, both major (tensile, positive) and minor (compressive, negative) strains are present. The highest absolute value was called maximum strain.

Data was analyzed in SAS 9.4. Proc Univariate analysis was used to verify normality of the variable and residuals. For statistical analysis, ordinary least squares regressions were run using Proc Reg, and

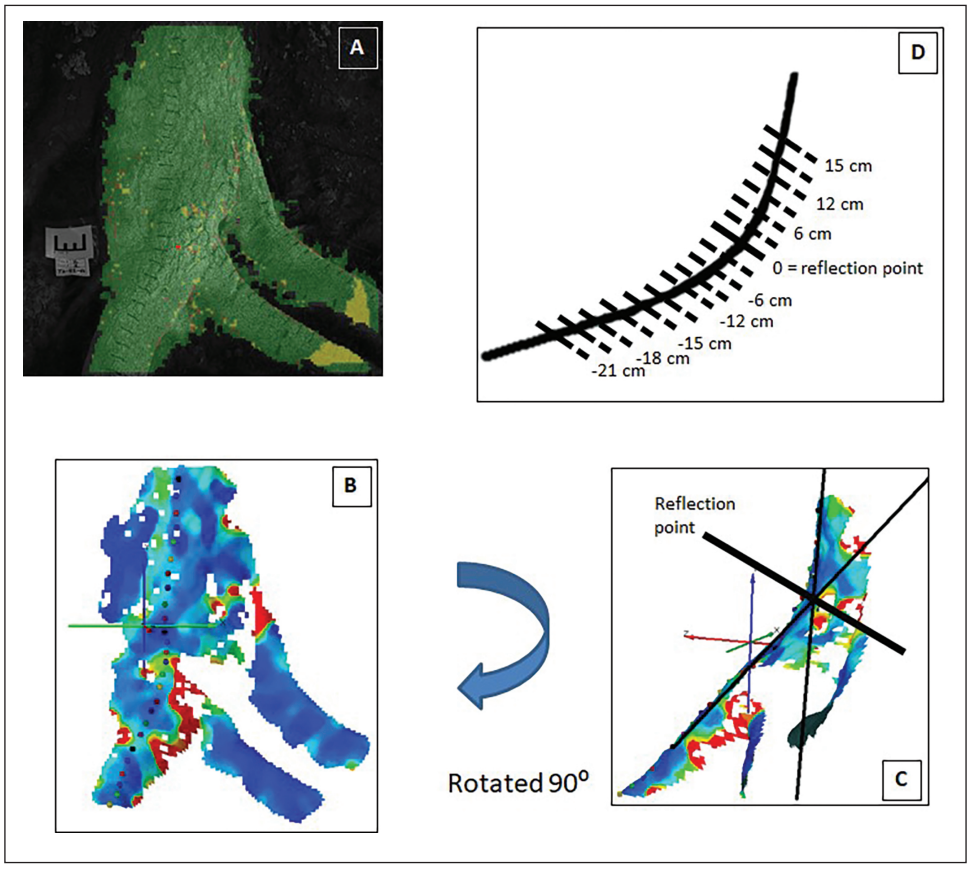

Figure 6. Root image with measurement area in green (A), strain map profile with dots as reference points (B), strain map rotated 90° to determine reflection point (C), and 3-cm demarcation from the reflection point (D).

ANOVAs were conducted with Proc GLM. Tukey's honest significant difference (HSD) was used for evaluating differences in mean values. Strain values were transformed using a reciprocal square root methodology to achieve normality. Data was back transformed after analysis for presentation purposes. All analyses used an alpha level of 0.05.

RESULTS

Mean (± SD) tree DBH was 51 ± 7 cm, and mean tree height ($Height_T$) was 19 ± 4 m. Pulling line height ($Height_A$) was 5.5 ± 1 m, and $Diam_A$ was 42 ± 7 cm. The maximum pulling force for sampled trees at 0.1° from natural lean was 18,537 ± 5,600 N and ranged from 6,436 to 30,234 N. The bending moment (M_{Bend}) for all pulls averaged 99,105 ± 40,435 Nm and ranged from 31,009 to 210,968 Nm.

The soil texture analysis performed on all the sampled trees indicated compacted soils near each sampled RSTZ orientation, with minimal O horizon formation (less than 0.5 cm). Initial soil ribbon tests found high percentages of clay (clay-loam and silty-clay) content within the undeveloped horizon at depths from 1 cm to 20 cm. These undeveloped soil horizons are indicative of soil found in areas that have been subjected to site modification for development purposes. The mean soil moisture was 36% ± 10%, and no statistically significant difference ($P = 0.250$) was found between the soil moisture for each root direction (leeward, windward, tangential).

For each of the 15 trees evaluated, the DIC measured strain at peak applied force at 8 to 10 locations designated along the line of reference marks (2.5-cm marks). A total of 133, 131, and 132 peak strain points were located within the defined RSTZ on the leeward orientation, on the windward orientation, and on the tangential orientation, respectively. Both tension (major) and compression (minor) strains were measured at any reference mark in all 3 root types. Leeward branches had compression as peak strain in

Table 1. Contribution of strain type to maximum strain at root-stem transition zones and respective orientation at peak applied load during static load tests.

Orientation	*n*	Strain type (% of location)	
		Tension	Compression
Leeward	133	3.8%	96.2%
Windward	131	95.4%	4.6%
Tangential	132	65.2%	34.8%

96.2% of the reference marks, windward roots had tensile strain in 95.4%, and tangential roots had a mix of both compression and tension strain (Table 1).

The 3 root types were not always directly in line with, or tangent to, the direction of pull. Overall mean root divergence from the direction of pull was 18.7°, and there was not a statistically significant difference between mean root divergence for the 3 root directions (P = 0.0649, n = 45). No significant relationships were identified between maximum strain and root divergence for leeward (r^2 = 0.04, n = 133), windward (r^2 = 0.01, n = 131), or tangential (r^2 = 0.01, n = 132) orientations. Significant linear regressions were not found between maximum strain and tree factors: DBH (r^2 = 0.01, n = 369), tree height (r^2 = 0.01, n = 369), peak load (r^2 = 0.02, n = 369), bending moment (r^2 = 0.02, n = 369), or soil moisture (r^2 = 0.02, n = 369).

Table 2. Mean maximum strain at the reflection point of the root curvature. Mean maximum strain with the same letter were not found to differ using a Tukey HSD comparison (alpha 0.05). Strain was analyzed at the inverse square root to correct for normality and presented as a back transformed number.

Orientation	*n*	Mean strain (%)
Leeward	15	0.0910a
Windward	15	0.0911a
Tangential	15	0.0492b
P-value		0.0012

No significant linear relationship was found between maximum strain and reference marks along the roots, whether overall (r^2 = 0.02, n = 396) or by root type leeward (r^2 = 0.04, n = 133), windward (r^2 = 0.01, n = 131), or tangential (r^2 = 0.01, n = 132). Mean maximum strain at the reflection point was found to be lowest in the tangential roots and larger in the leeward and windward roots (P = 0.0012, n = 45, Table 2).

Strain regressed against bending moment reflection point at the 5 time intervals was found to have a logarithmic relationship with bending moment for leeward (r^2 = 0.27, n = 75, Figure 7) and windward (r^2 = 0.29, n = 75, Figure 8) orientations. A weaker logarithmic relationship, however, was found for tangential roots (r^2 = 0.197, n = 75, Figure 9).

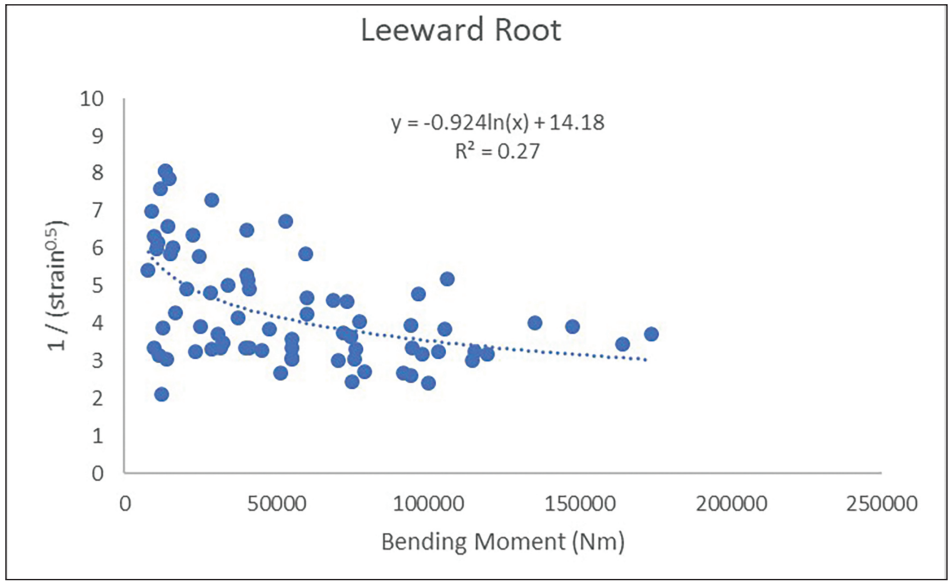

Figure 7. Logarithmic relationship between bending moment and strain (1/strain$^{0.5}$) in leeward roots reflection point. The transformed inverse of the square root of strain is plotted in the graph.

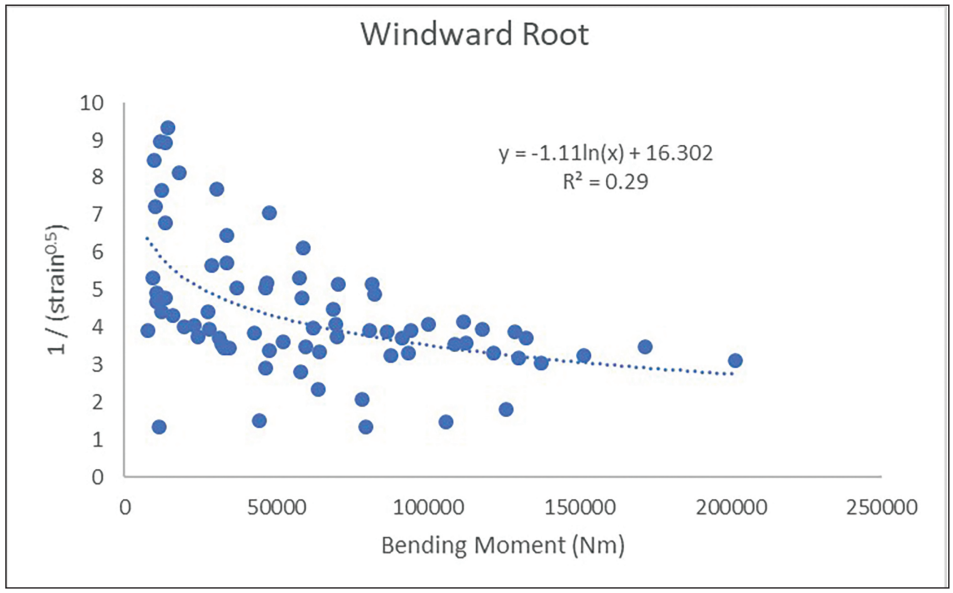

Figure 8. Logarithmic relationship between bending moment and strain (1/strain$^{0.5}$) in windward roots reflection point. The transformed inverse of the square root of strain is plotted in the graph.

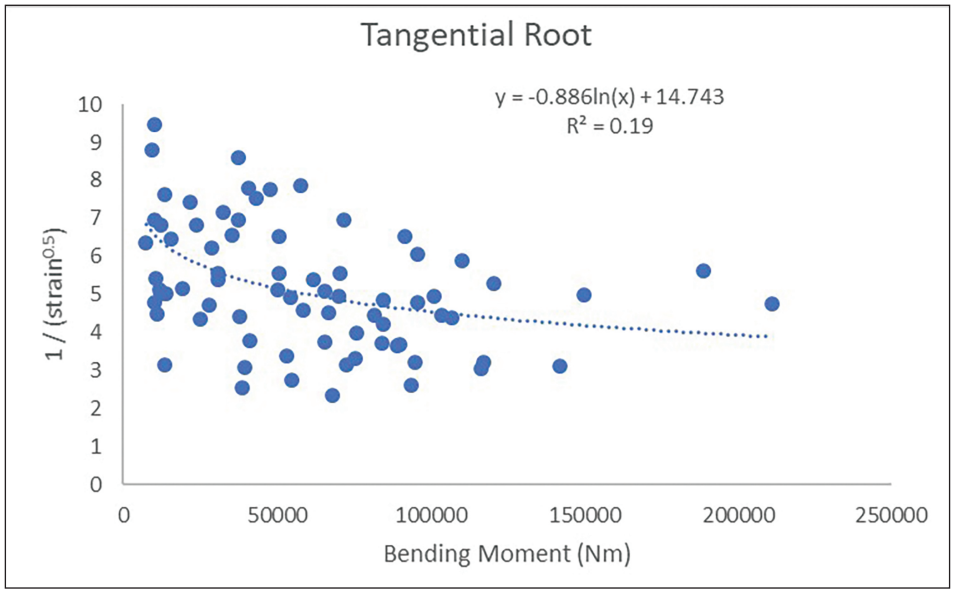

Figure 9. Logarithmic relationship between bending moment and strain (1/strain$^{0.5}$) in tangential roots reflection point. The transformed inverse of the square root of strain is plotted in the graph.

DISCUSSION

Our static load trials subjected 15 trees to a static bending force that caused a minor 0.1° deflection. These tests indicated that strain patterns on the leeward RSTZ orientation were primarily comprised of compressive (minor) strains, while the windward roots developed tensile strain within the first meter of roots. These types of strain concentrations are comparable to relevant research that indicate leeward wood fibers of trees subjected to loading are held in compression, while windward wood fibers are more in tension under loading (Stokes 1999).

While the type of strain on the leeward and windward roots was different, the magnitude was found to be the same at 0.091%, while strain in the tangential roots was 53% lower at 0.049%. These findings suggest that the roots in line with the direction of the static pull were subjected to nearly twice the loading as that of the tangential roots. Whether this pattern of strain and thus load distribution will continue through the zone of rapid taper was not determined. Additionally, since these trials only induced a minor tilt (0.1°), whether the difference in strain in tangential roots and those in line with the direction of loading will remain similar to our findings for heavier or extreme loading events is unknown.

Strain being lower in the tangential roots is likely the result of these roots being more in line with the neutral plane of loading. The type of strain in the tangential roots was not consistent, as 65% were tensile strain and 35% were compressive strain (Table 1). These strain patterns found on the tangential RSTZ orientation could indicate torsional stress or shear plane stress were developing in tree roots subjected to unidirectional loading (Neild and Wood 1999; James et al. 2013a, 2013b). However, we were not able to determine anchoring strength or full root morphology properties that could impact strain transmission in our roots. As torsional strain is often disregarded during loading trials (Dahle and Grabosky 2012), we believe the data in this study suggests it may be worth designing a study to measure the impact of torsional and/or shear stress in roots.

The ability to utilize DIC to measure strain directly on bark and infer strain in the xylem has been called into question. Dahle (2017) did not find differences between strain values of xylem and bark in thin barked samples, while Sebera et al. (2014, 2016) found differences at higher loads in thicker trees with thick bark. However, for this research, we are primarily concerned with mapping strain patterns along a relatively concentrated portion of the RSTZ and not in determining strain values at failure. Strain in this region was found to increase with bending moment and suggests that mapping strain on the bark was reasonable with the minor loading that took place in this study. The strain values in our study were lower than those reported in roots during failure exercises (Stokes 1999) using strain gauges. However, our study was not designed to compromise the stability of the trees or determine strain values at the point of failure. For this study, we were interested in determining the overall patterns of strain movement, thus inferring how load is transferred from the stem into the roots. Bark deformation must follow a similar pattern as the xylem, or there would be separation of these two tissues causing death of the cambium (Dahle 2017). Indeed, there are patterns of hydro-elastic swelling or shrinkage and the day-night expansion or shrinkage of bark (Bonnesoeur et al. 2016), during which the tree must maintain the connection between these tissues. While the total magnitude of strain may be slightly different along the bark compared to the xylem, we believe the overall patterns are valid. This study demonstrated the potential application of DIC in the biological research and arboricultural management fields to nondestructively test and monitor trees in their natural environment.

Surprisingly, strain was not found to vary in quantity along the demarcated region of the RSTZ, therefore suggesting that loading is consistent in the region of study on any given root or into the beginning of the trunk. However, we were not able to measure strain deeper into the zone of rapid taper, so we are unsure of the mechanisms and magnitude that strain may dissipate as the loading moves distally along a root.

The relative low values for strain in this study are the result of only inducing a minor static pull. A concern during the initial design of this study was that the static pulls would lead to tree instability. James et al. (2013a) found that a stem inclination of 0.9° can lead to root damage, and instability may be induced in as little as a 0.25° inclination (Brudi and van Wassenaer 2002). As such we set an inclination limit of 0.1° so that the stability of the trees was not impacted by our tests. An additional concern was staying below the maximum elastic limit for the pin oak species (0.62). Since we pulled multiple times per tree, each tree may need to relax between pulls to return to the original

state. At least 10 minutes elapsed between subsequent pulls on the same root and at least 20 minutes between pulls on roots when moving to the next sampled root. A strong relationship between bending moment and DBH (reported in Beezley et al. 2016) indicates that the trees relaxed between pulls.

CONCLUSIONS

Efforts to quantify the structural stability of trees are actively being pursued by the arboricultural practitioner and research community. Current tree risk assessments may not fully consider the long-term responses of trees to mechanical stress, and thus many large amenity trees may have been prematurely felled in hopes of diverting litigious citations and compromising public safety. Mechanical stress is induced within trees during dynamic and static loading events. This loading can cause failure in both aboveground and belowground portions of a tree. Understanding how the load is transferred through the RSTZ, and if the resulting force is evenly dispersed throughout the root zone, can be an important consideration, especially if damage occurs to a specific section of the roots. Understanding how load and resulting strains move from the stem through the RSTZ into the root system and finally into the soil is important for better understanding tree stability. This study demonstrates that DIC can be successfully utilized to map strain in urban tree roots. Researchers can now consider using DIC to investigate how strain moves out from the RSTZ into the structural and smaller roots and potentially into the soil.

Researchers have noted the importance of understanding how forces move through trees and finding methods to assess the stability of trees (Dahle et al. 2014). Understanding that loading results in significantly higher strains on in-line roots, rather than tangential roots, has important management implications. Specifically, severing roots in line with the prevailing direction of wind or other loads will lead to reduced tree stability. This finding, however, does not diminish the importance of the tangential sides of the tree and the effects of torsion within the structural root system. Further research is needed to fully understand the implications of loading on tangential root systems.

LITERATURE CITED

Beezley K, Dahle G, Miesbauer J. 2016. Strain measurement within trees across the root-stem transition zone (RSTZ). *Proceedings of the 11th international symposium on environmental concerns in rights-of-way management*; Halifax, CA, USA. p. 107-114.

Beezley K, Dahle G, Miesbauer J, Walker M. 2020. Importance of the root-stem transition zone in the stability of trees. In: Watson G, Gilman E, Miesbauer J, Morgenroth J, Scharenbroch B, editors. *Landscape below ground IV: proceedings of the fourth international workshop on tree root development in urban soils*. Atlanta (GA, USA): International Society of Arboriculture. p. 300-315.

Bonnesoeur V, Constant T, Moulia B, Fournier M. 2016. Forest trees filter chronic wind-signals to acclimate to high winds. *New Phytologist*. 210(3):850-860.

Brudi E, van Wassenaer PJ. 2002. Trees and statics: nondestructive failure analysis. In: Coder KD, Smiley ET, editors. *Tree structure and mechanics conference proceedings: how trees stand up and fall down*. Champaign (IL, USA): International Society of Arboriculture. p. 53-70.

Burgert I. 2006. Exploring the micromechanical design of plant cell walls. *American Journal of Botany*. 93:1391-1401.

Coder K. 2008. Storm wind loads and tree damage. Athens (GA, USA): Warnell School of Forestry and Natural Resources, the University of Georgia. WSF&NR08-24. 35 p.

Coutts MP. 1983. Root architecture and tree stability. *Plant and Soil*. 71:171-188.

Dahle GA. 2017. Influence of bark on the measurement of mechanical strain using digital image correlation. *Wood Science and Technology*. 51:1469-1477.

Dahle GA, Grabosky JC. 2009. Review of literature on the function and allometric relationships of tree stems and branches. *Arboriculture & Urban Forestry*. 35:311-320.

Dahle GA, Grabosky JC. 2010. Variation in modulus of elasticity (*E*) along *Acer platanoides* L. (*Aceraceae*) branches. *Urban Forestry & Urban Greening*. 9:227-233.

Dahle GA, Grabosky JC. 2012. Determining if lateral imbalance exists in first-order branches leading to a potential development of torsional stress. *Arboriculture & Urban Forestry*. 38(4): 141-145.

Dahle GA, Grabosky J, Kane B, Miesbauer J, Peterson W, Telewski FW, Koeser A, Watson GW. 2014. Tree biomechanics: a white paper from the 2010 international meeting and research summit at The Morton Arboretum (Lisle, Illinois, U.S.). *Arboriculture & Urban Forestry*. 40:309-318.

Dahle GA, James KR, Kane B, Grabosky JC, Detter A. 2017. A review of factors that affect the static load-bearing capacity of urban trees. *Arboriculture & Urban Forestry*. 43(3):89-106.

Dupuy L, Fourcaud T, Stokes A. 2005. A numerical investigation into the influence of soil type and root architecture on tree anchorage. *Plant and Soil*. 278:119-134.

Esau K. 1977. *Anatomy of seed plants*. 2nd Ed. New York (NY, USA): John Wiley & Sons. p. 61-181.

Fayle DC. 1983. Differences between stem and root thickening at their junction in red pine. *Plant and Soil*. 71:161-166.

Genet M, Stokes A, Salin F, Mickovski S, Fourcaud T, Dumail J, Beek R. 2005. The influence of cellulose content on tensile strength in tree toots. *Plant and Soil*. 278:1-9.

Gibbs JN, Greig BJW. 1990. Survey of parkland trees after the great storm of October 16, 1987. *Arboricultural Journal*. 14:321-347.

Hale S, Gardiner B, Wellpott A, Nicoll B, Achim A. 2010. Wind loading of trees: influence of tree size and competition. *European Journal of Forest Research*. 131:203-217.

James K. 2003. Dynamic loading of trees. *Journal of Arboriculture*. 29:165-171.

James KR, Dahle GA, Grabosky J, Kane B, Detter A. 2014. Tree biomechanics literature review: dynamics. *Arboriculture & Urban Forestry*. 40:1-15.

James K, Hallam C, Spencer C. 2013a. Measuring tilt of tree structural root zones under static and wind loading. *Agricultural & Forest Meteorology*. 168:160-167.

James K, Hallam C, Spencer C. 2013b. Tree stability in winds: measurements of root plate tilt. *Biosystems Engineering*. 115:324-331.

James KR, Haritos N, Ades PK. 2006. Mechanical stability of trees under dynamic loads. *American Journal of Botany*. 93:1522-1530.

James KR, Moore JR, Slater D, Dahle GA. 2018. Tree biomechanics. *CAB Reviews*. 12(38):1-11.

Jonsson MJ, Foetzki A, Kalberer M, Lundsrom T, Ammann W, Stockli V. 2006. Root-soil rotation stiffness of Norway spruce (*Picea abies* (L.) Karst) growing on subalpine forested slopes. *Plant Soil*. 285:267-277.

Kane B. 2014. Determining parameters related to the likelihood of failure of red oak (*Quercus rubra* L.) from winching tests. *Trees*. 28:1667-1677.

Kane B, Clouston P. 2008. Tree pulling tests of large shade trees in the genus *Acer*. *Arboriculture & Urban Forestry*. 34:101-109.

Kozlowski T, Pallardy S. 1997. *Physiology of woody plants*. 2nd Ed. San Diego (CA, USA): Academic Press. 411 p.

Lyford WH, Wilson BF. 1964. Development of the root system of *Acer rubrum* L. Petersham (MA, USA): Harvard University. Harvard Forest Paper No. 10. 20 p.

Moore GM. 2014. Wind-thrown trees: storms or management? *Arboriculture & Urban Forestry*. 40:53-69.

Moore JR, Maguire DA. 2004. Natural sway frequencies and damping ratios of trees: concepts, review and synthesis of previous studies. *Trees*. 18:195-203.

Neild SA, Wood CJ. 1999. Estimating stem and root-anchorage flexibility in trees. *Tree Physiology*. 19:141-151.

Niklas KJ. 1992. *Plant mechanics: an engineering approach to plant form and function*. Chicago (IL, USA): The University of Chicago Press. 607 p.

Niklas KJ. 2002. Wind, size, and tree safety. *Journal of Arboriculture*. 28:84-93.

Peltola HM. 2006. Mechanical stability of trees under static loads. *American Journal of Botany*. 93:1501-1511.

Sebera V, Kunecky J, Praus K, Tippner J, Horacek P. 2016. Strain transfer from xylem to bark surface analyzed by digital image correlation. *Wood Science and Technology*. 50:773-787.

Sebera V, Praus L, Tippner J, Kunecky J, Cepela J, Wimmer R. 2014. Using optical full-field measurement based on digital image correlation to measure strain on a tree subjected to mechanical load. *Trees*. 28:1173-1184.

Smiley ET, Holmes L, Fraedrich BR. 2014. Pruning of buttress roots and stability changes of red maple (*Acer rubrum*). *Arboriculture & Urban Forestry*. 40:230-236.

Stokes A. 1999. Strain distribution during anchorage failure of *Pinus pinaster* Ait. at different ages and tree response to wind-induced root movement. *Plant and Soil*. 217:17-27.

Yang M, Défossez P, Danjon F, Fourcaud T. 2014. Tree stability under wind: simulating uprooting with root breakage using a finite element method. *Annals of Botany*. 114:695-709.

ACKNOWLEDGMENTS

This research was funded in part by NIFA through the McIntire Stennis Program Project #WVA00125, a Tree Fund Duling Grant 14-JD-02, WVU Davis College Division of Forestry & Natural Resources, and The Morton Arboretum. We would like to thank Sam Adams (currently with the WV Division of Forestry Urban & Community Forestry Program) for helping collect the data, as well as Tom Smiley (Bartlett Tree Research Laboratory) and Matt Melis (NASA Glenn Research Center) for developing the initial idea for this research at Biomechanics Week 2013.

Kenneth E. Beezley
West Virginia University
Division of Forestry and Natural Resources
Morgantown, WV, USA

Gregory A. Dahle (corresponding author)
West Virginia University
Division of Forestry and Natural Resources
Morgantown, WV, USA
gregory.dahle@mail.wvu.edu

Jason Miesbauer
The Morton Arboretum
Lisle, IL, USA

David DeVallance
InnoRenew CoE
Izola, Slovenia
University of Primorska
Koper, Slovenia

Conflicts of Interest:
The authors reported no conflicts of interest.

Résumé. Les arbres réagissent à des charges mécaniques pendant toute leur durée de vie sinon ils risquent une mortalité prématurée. La contrainte résultant des charges interceptées par la canopée et répercutées à travers l'arbre est d'une importance significative, non seulement pour la survie de l'arbre, mais pour la sécurité et le bien-être de la population humaine avoisinante. Dans le but de tester la fonction de l'orientation de l'arbre par rapport à une charge appliquée, des tests de charge statique furent menés sur 15 chênes des marais matures (*Quercus palustris* Muenchh.). Nous avons appliqué les tests de charge statique pour incliner les arbres de 0.1° par rapport à leur position naturelle. Nous avons utilisé un système de corrélation d'images numériques pour cartographier les contraintes sous le vent, du côté du vent ainsi que les racines tangentielles dans la zone de transition entre

la racine et la tige. Les résultats montrèrent que les amplitudes maximales moyennes des contraintes étaient similaires tant pour les orientations sous le vent que du côté de celui-ci, et plus basses pour l'orientation tangentielle. L'orientation sous le vent a subi une contrainte de compression tandis que l'orientation du côté du vent a expérimenté une contrainte de traction alors que l'orientation tangentielle a subi à la fois une contrainte de traction et de compression. Ces informations fournissent aux secteurs de l'arboriculture et des sciences végétales une meilleure compréhension sur la manière dont les charges se répartissent dans les arbres et amélioreront encore l'évaluation des risques pour les arbres et les protocoles de gestion de la zone racinaire.

Zusammenfassung. Bäume sind während ihrer Lebensdauer mechanischen Belastungen ausgesetzt oder sind gefährdet vorzeitig zu sterben. Die Beanspruchung, die sich aus der Last ergibt, die von der Baumkrone abgefangen und auf den gesamten Baum übertragen wird, ist von erheblicher Bedeutung. Nicht nur für das Überleben des Baumes, sondern auch für die Sicherheit und das Wohlbefinden der Menschen, die sich in unmittelbarer Nähe befinden. Um die Funktion der Ausrichtung des Baumes auf eine einwirkende Last zu testen, wurden statische Belastungstests an 15 ausgewachsenen Pinieneichen (*Quercus palustris* Muenchh.) durchgeführt. Wir haben die statischen Belastungstests angewendet, um die Bäume um 0.1° aus der natürlichen Position zu kippen. Wir verwendeten ein digitales Bildkorrelationssystem, um die Dehnung in der Lee-, Luv- und Tangentialwurzel in der Wurzel-Schaft-Übergangszone abzubilden. Die Ergebnisse deuten darauf hin, dass die maximalen Dehnungswerte in der Lee- und Luvorientierung ähnlich und in der tangentialen Orientierung niedriger sind. In der Leeorientierung wurden Druckspannungen, in der Luvorientierung Zugspannungen und in der tangentialen Orientierung sowohl Zug- als auch Druckspannungen gemessen. Diese Informationen liefern den Sektoren Baumzucht und Pflanzenwissenschaften ein besseres Verständnis darüber, wie sich die Belastungskraft durch die Bäume verlagert. Außerdem werden sie die Protokolle zur Risikobewertung von Bäumen und zum Wurzelzonenmanagement weiter verbessern können.

Resumen. Los árboles se someten a una carga mecánica durante su vida útil o se enfrentan a la mortalidad prematura. La tensión resultante de las cargas interceptadas por el dosel y transferidas por todo el árbol es de gran importancia, no sólo para la supervivencia del árbol, sino para la seguridad y el bienestar de la población humana que se encuentra en las proximidades. Para probar la función de orientación del árbol a una carga aplicada, se realizaron pruebas de carga estática en 15 robles maduros (*Quercus palustris* Muenchh.). Aplicamos las pruebas de carga estática para inclinar los árboles 0.1° desde la posición natural. Usamos un sistema de correlación de imágenes digitales para mapear en orientación de sotavento, barlovento y tangencial en la zona de transición del tallo de la raíz. Los resultados indican que las magnitudes de deformación unitaria máxima media son similares en las orientaciones sotavento y barlovento e inferiores en la orientación tangencial. La orientación sotavento experimentó tensión compresiva, la orientación barlovento experimentó tensión y la orientación tangencial tenía las dos: tensión y compresión. Esta información proporciona a los sectores de la ciencia arbocultural y de las plantas una mejor comprensión de cómo se mueven las fuerzas de carga a través de los árboles y mejorará aún más la evaluación del riesgo de los árboles y los protocolos de gestión de las zonas radiculares.

Arboriculture & Urban Forestry Quiz Questions

To complete this quiz, go to the ISA website, log into your MyISA account, and make your way to the page for *Arboriculture & Urban Forestry* CEU Quizzes (www.isa-arbor.com/store/ceuquizzes/113).

Add the quiz to your cart, proceed through checkout, and look for the content to appear on your personal dashboard under the header, "My Quizzes." If you need a username and password, send us an e-mail (isa@isa-arbor.com).

A passing score for this quiz requires sixteen correct answers. Quiz results will display immediately upon quiz completion. CEU(s) are processed immediately. You may take the quiz as often as is necessary to pass.

CEU quiz by Eric North, University of Nebraska-Lincoln, Lincoln, Nebraska, USA